Theoretical analysis of Cherenkov third harmonic generation via two cascaded $^{(2)}$ processes in a waveguide

2014 Laser Phys. 24 105404

(http://iopscience.iop.org/1555-6611/24/10/105404)

IOP Publishing | Astro Ltd Laser Physics
Laser Phys. **24** (2014) 105404 (6pp) doi:10.1088/1054-660X/24/10/105404

Theoretical analysis of Cherenkov third harmonic generation via two cascaded $\chi^{(2)}$ processes in a waveguide

C D Chen[1] **and X P Hu**[2]

[1] College of Science, Nanjing University of Aeronautics and Astronautics, Nanjing 211100, People's Republic of China
[2] National Laboratory of Solid State Microstructures, Nanjing University, Nanjing, 210093, People's Republic of China

E-mail: cdchen@nuaa.edu.cn

Received 12 June 2014, revised 4 July 2014
Accepted for publication 5 July 2014
Published 22 August 2014

Abstract

We report a comprehensive numerical study of a type of quasi-phase-matched Cherenkov third harmonic generation in a nonlinear waveguide, and this Cherenkov third harmonic generation consists of a guided-to-guided second harmonic generation cascaded with a guided-to-radiated sum-frequency generation. Following the coupled-mode theory, the temperature-detuning characteristics of third harmonic (TH) radiation under different pumping-power densities were studied. TH power dependences on interaction length have been discussed as well, which includes three situations: without reciprocal vector participating, and forward and backward reciprocal vector participating. In addition, we demonstrate that the Cherenkov angle of each TH radiation is not sensitive to the temperature variation.

Keywords: waveguide, frequency conversion, nonlinear Cherenkov radiation

(Some figures may appear in colour only in the online journal)

1. Introduction

Non-linear Cherenkov radiation (NCR) may occur when the non-linear polarization wave has a faster phase velocity ($\overrightarrow{v_p}$) than that of a free wave at the harmonic in the medium [1]. In recent years, there has been increasing interest in the study of NCR in optical materials. Varieties of research on Cherenkov second harmonic generation (SHG) [2–7], sum-frequency generation (SFG) [8–12] and difference-frequency generation [13] have been reported. More recently, Cherenkov third harmonic generation (CTHG) has also been experimentally realized in both quasi-phase-matched (QPM) waveguide systems [14] and bulk photonic crystal systems [15–17]. Considering the rather small $\chi^{(3)}$ of $LiTaO_3$ or $LiNbO_3$ crystals, in these cases, they both adopted two cascaded $\chi^{(2)}$ processes to realize such radiations. The difference between these two systems is that the fundamental wave and the second harmonic wave are non-collinear in bulk crystals, although they are collinear in the non-linear waveguide. The waveguide CTHG consists of the following two second-order non-linear processes: a guided-to-guided SHG process cascaded with a guided-to-radiated SFG process. In the first waveguide SHG procedure between discrete guided modes, the phase-matching condition is strict, and its conversion efficiency can be greatly enhanced using QPM structures, thus providing enough second harmonic (SH) waves to carry out the cascaded guided-to-radiated SFG process. The Cherenkov SFG process can be automatically phase-matched transversely, and the radiations can be modulated by the involved reciprocal vectors. The energy of the guided fundamental and SH waves partially generate a group of third harmonic (TH) radiated modes that emit into the substrate. In previous years, some excellent theoretical works about Cherenkov SHG [18, 19] have been reported. However, so far there have been few detailed theoretical studies on QPM CTHG via two cascaded $\chi^{(2)}$ processes.

In this paper, we proposed a simple computational model and used the non-linear coupled-mode equations to present a detailed study of CTHG, which comprises two cascaded $\chi^{(2)}$

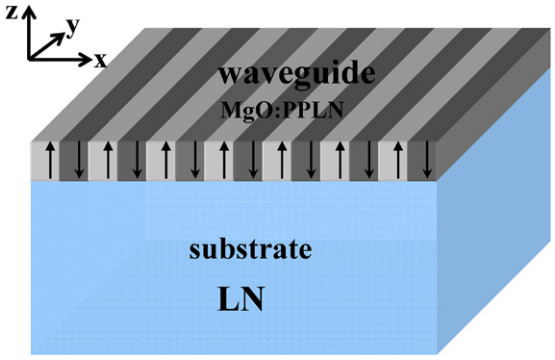

Figure 1. The waveguide configuration for qui-phase matching Cherenkov third harmonic generation. '↑' and '↓' represent the positive and negative domains in the periodically-poled waveguide, respectively.

procedures in a periodically poled MgO:$LiNbO_3$ planar waveguide, with $LiNbO_3$ (LN) as the substrate. Temperature detuning curves at different pump power and TH power dependence on interaction length were studied. Other numerical results pertaining to CTHG were demonstrated as well.

2. Model and coupled-mode theory

The waveguide configuration is shown in figure 1. The waveguide layer is a z-cut 4 μm-thick periodically poled MgO:LN with a domain period of 14.6 μm, which has a reversal factor of 0.38, and is bonded to another congruent LN substrate. This domain-reversed structure is designed for frequency doubling of 1342 nm at 115° C. The phase-matching conditions of the two cascaded processes in CTHG can be expressed as

$$\left|2\vec{\beta_\omega} + \vec{G}_{\mathrm{m}}\right| = \left|\vec{\beta}_{2\omega}\right| \tag{1}$$

for waveguide SHG and

$$\left|\vec{\beta_\omega} + \vec{\beta}_{2\omega} + \vec{G}_{\mathrm{n}}\right| = |n_{\mathrm{e}}(3\omega)\vec{k}_0(3\omega)|\cos\theta \tag{2}$$

for Cherenkov SFG, in which $\vec{\beta_\omega}$ and $\vec{\beta}_{2\omega}$ are the propagation constants of TM_0 modes of the pump and SH wave, respectively. $G_{\mathrm{m}(n)} = \mathrm{m}(n)\cdot 2\pi/\Lambda$ is the $m(n)$th reciprocal vector of the periodic structure, $n_e(3\omega)$ is the extraordinary refractive index of the TH wave in substrate, $\vec{k}_0$ is the free-space wave vector, and θ is the Cherenkov angle. The pump and SH waves are considered to be guided TM modes, and the TH waves are in the form of a superposition of substrate TM radiation modes.

For this waveguide configuration, the optical field is confined in z-direction and propagates along x-direction. We define $A_\omega(x)$ and $A_{2\omega}(x)$ as the x-dependent amplitude of the guided modes at pump and SH, respectively. Although the radiation modes in the waveguide are continuous, the special radiated mode has the fixed propagation constant. So $A_{3\omega}(\beta_{3\omega}, x)$ is used as the amplitude of the TH radiation mode with propagation constant $\beta_{3\omega}$. Following the coupled-mode theory, we could get three coupled-wave equations, as below:

$$\frac{dA_\omega(x)}{dx} = -i\omega\left[\kappa_1 A_{2\omega}A_\omega^*\exp(-i\Delta\beta_1 x) + \kappa_2\int A_{3\omega}(\beta_{3\omega}, x)\exp(i\Delta\beta_2 x)d\beta_{3\omega}\cdot A_{2\omega}^* - 0.5\alpha_1 A_\omega\right] \tag{3}$$

$$\frac{dA_{2\omega}(x)}{dx} = -2i\omega\left[0.5\cdot\kappa_1 A_\omega^2\exp(-i\Delta\beta_1 x) + \kappa_2\int A_{3\omega}(\beta_{3\omega}, x)\exp(i\Delta\beta_2 x)d\beta_{3\omega}\cdot A_\omega^*\right] - 0.5\alpha_2 A_{2\omega} \tag{4}$$

$$\frac{dA_{3\omega}(x)}{dx} = -3i\omega\kappa_2 A_{2\omega}A_\omega\exp(i\Delta\beta_2 x) - 0.5\alpha_3 A_{3\omega} \tag{5}$$

in which

$$\kappa_1 = 2d_{33}g_1\sqrt{\frac{2\mu_0}{cn_1{}^2n_2\gamma_1}} \tag{6}$$

and

$$\kappa_2 = 2d_{33}g_2\sqrt{\frac{2\mu_0}{cn_1n_2n_3\gamma_2}} \tag{7}$$

are the coupling coefficients of waveguide SHG and Cherenkov SFG processes, respectively. n_1 and n_2 are the effective refractive indexes of the pump and SH in the waveguide, respectively, n_3 is the refractive index of the TH in substrate, and g_1 and g_2 are Fourier coefficients in the SHG and SFG processes. $\Delta\beta_1$ and $\Delta\beta_2$ are the phase-mismatching in the SHG and CTHG processes, α_1, α_2 and α_3 are the linear power-loss coefficients of the pump, SH and TH waves. γ_1 and γ_2 are the effective cross-sectional area of waveguide in the guided-to-guided SHG process and guided-to-radiated SFG process, respectively, which could be defined as below:

$$\gamma_1 = \frac{\left(y\cdot\int|\Phi_1|^2dz\right)^2\cdot y\cdot\int|\Phi_2|^2dz}{\left(y\cdot\int\Phi_2{}^*\Phi_1{}^2dz\right)^2} \tag{8}$$

$$\gamma_2 = \frac{\left(y\cdot\int|\Phi_1|^2\mathrm{d}z\right)\cdot\left(y\cdot\int|\Phi_2|^2\mathrm{d}z\right)\cdot\left(y\cdot\int|\Phi_3|^2\mathrm{d}z\right)}{\left(y\cdot\int\Phi_3{}^*\Phi_2\Phi_1\mathrm{d}z\right)^2} \tag{9}$$

in which y is the beam width of the pump; Φ_1, Φ_2 and Φ_3 are field distributions of the guided pump, SH modes and TH radiated mode, respectively. The propagation constants of radiation modes are continuum, but the corresponding field distribution for a particular radiated mode has a single value of propagation constant. Since Cherenkov radiation is automatically phase-matched transversely, the radiated TH can fully emit into substrate via an adjustable angle referring to $\Delta\beta_2 \to 0$, which leads to a maximum TH intensity under the corresponding conditions.

3. Results and discussion

In the simulations, the crystal length was 10 mm; $\alpha 1$, $\alpha 2$ and $\alpha 3$ were set to be 0.002 cm^{-1}, 0.025 cm^{-1}, 0.025 cm^{-1} [20],

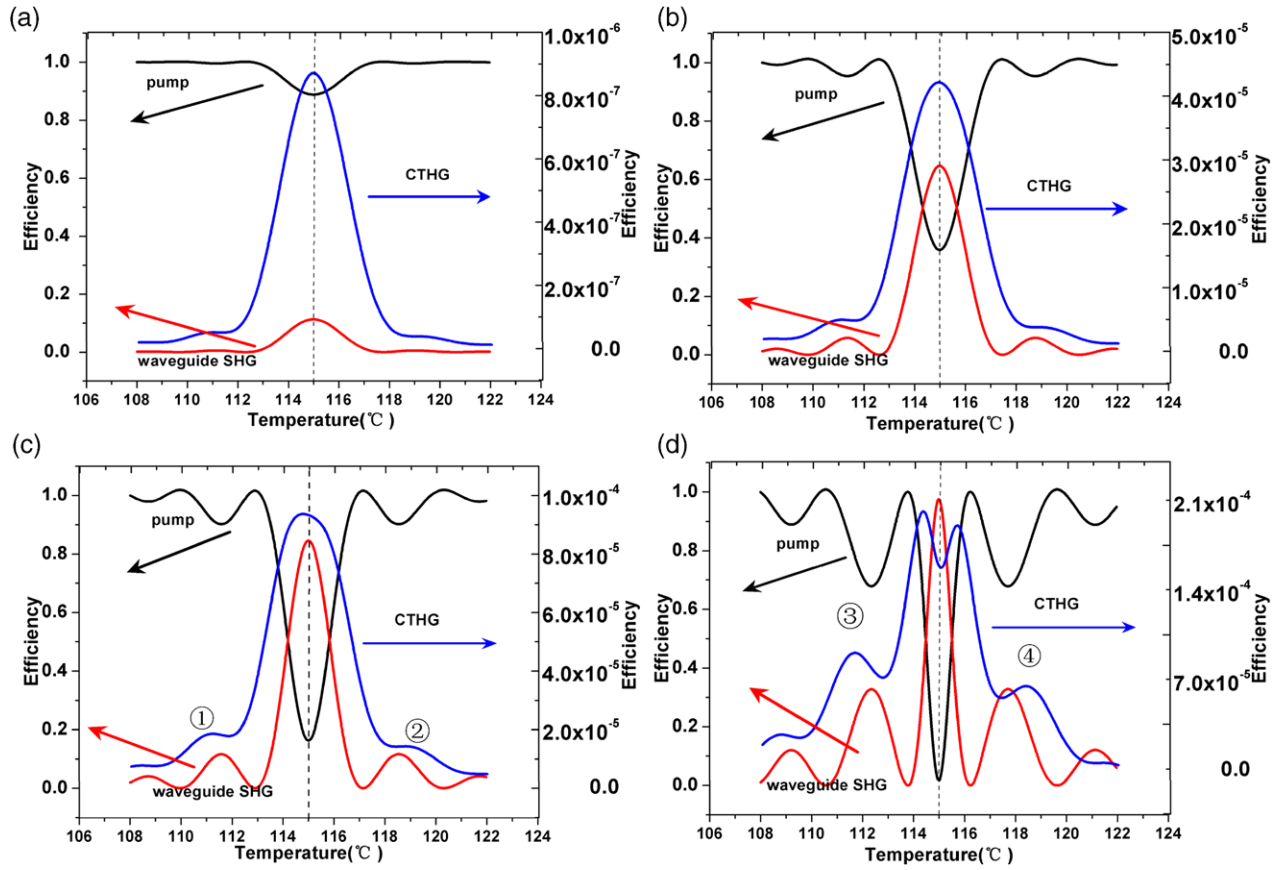

Figure 2. For the case without reciprocal vector involved in Cherenkov sum-frequency generation process, temperature detuning curves of the pump, second harmonic and third harmonic waves under different pump power densities: (*a*) 0.2 MW cm^{-2}, (*b*) 2 MW cm^{-2},(*c*) 4 MW cm^{-2} and (*d*) 12 MW cm^{-2}.

respectively. For CTHG without reciprocal vectors participating in SFG process, when the pump power densities were set to be 0.2 MW cm^{-2} and 2 MW cm^{-2}, the temperature-detuning curves in these two cases had similar trends, which are shown in figures 2(*a*) and (*b*). We could see that the radiated TH intensity increased with the waveguide SH intensity, and they both reached the peaks at 115° C. When the pump power intensity was increased to 4 MW cm^{-2}, as shown in figure 2(*c*), the TH intensity reached the maximum at a temperature that was slightly lower than that of the SHG, which can be seen more clearly in figure 2(*d*) at a pump power density of 12 MW cm^{-2}. Actually, TH efficiency was affected by the pump and SH power together. Although there was a rather high SHG efficiency, seeing figure 2(*d*), the pump power had a large depletion as to create a dip of TH power where the SH power was the largest. From figures 2(*a*) to (*d*), it was found that the bandwidth of SH declined gradually with the increase of pump power, while TH bandwidths nearly remained unchanged at different pump powers. Considering the case that reciprocal vectors were involved in the cascaded process, we also studied their temperature characteristics of TH, which included reciprocal vectors $\vec{G}_1$ and $\vec{G}_{-1}$ shown in figure 3. It was found that the temperature bandwidth became smaller slightly and the other performances were similar to the case without any reciprocal vectors.

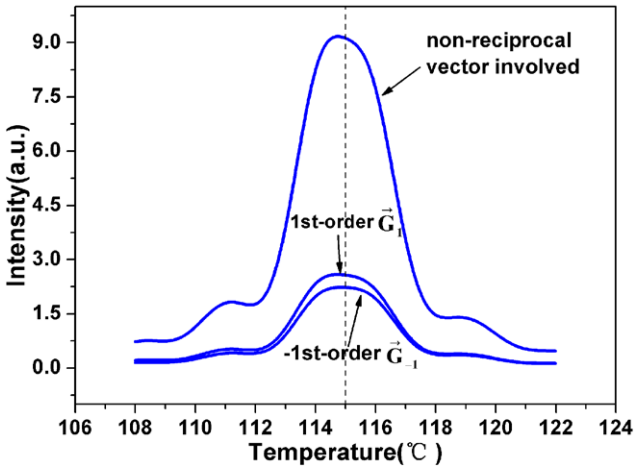

Figure 3. The temperature detuning curves of third harmonic radiations at a pumping power of 4 MW cm^{-2} for three cases: without reciprocal vector involved, reciprocal vectors $\vec{G}_1$ and $\vec{G}_{-1}$ involved.

With a careful observation of figure 2 or figure 3, one could see that the TH temperature-detuning curves had no bilateral symmetry with the dash lines at 115° C, especially in figures 2(*c*) and (*d*), which was distinct from that of the SH curves. The reason for this asymmetry mainly lay in the different overlapping dependences on the temperature. As

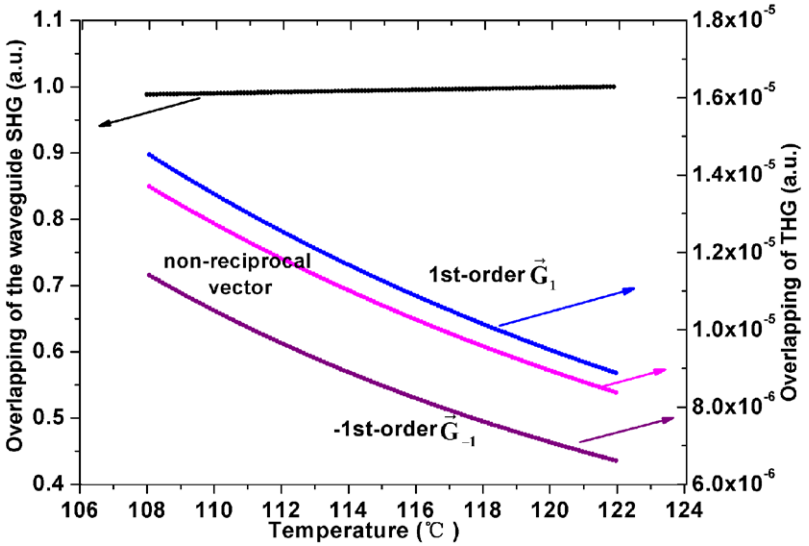

Figure 4. The mode overlapping dependences on temperature in waveguide SHG and CTHG processes. For CTHG, it includes the cases without reciprocal vector involved, forward and backward reciprocal vectors $\vec{G}_1$ and $\vec{G}_{-1}$ involved, respectively.

shown in figure 4, the overlapping in waveguide SHG was almost immutable with the variances in temperature, so the SH temperature-detuning curves were of symmetry with the dash lines. However, the overlapping in CTHG, including the three cases above, all decreased with the increase in temperature, which resulted in the higher TH efficiency at a lower temperature under the same pump and SH power conditions, such as 1, 2 in figure 2(*c*) and 3, 4 in figure 2(*d*).

Compared with the intensity of TH radiations, Cherenkov angles have some distinct characteristics. Theoretically, the Cherenkov angle θ_c^{out}(out of the crystal) satisfies the equations as below:

$$|\vec{k}(3\omega)|\cdot\cos\theta_c^{\text{in}} = \left|n_{\text{LN:Mg}}(T,\omega)\cdot\vec{k}(\omega) + n_{\text{LN:Mg}}(T,2\omega)\cdot\vec{k}(2\omega) + \vec{G}_m\right| \quad (10)$$

$$\sin\theta_c^{\text{out}} = n_{\text{LN}}(T,3\omega)\cdot\sin\theta_c^{\text{in}} \quad (11)$$

in which T is defined as temperature; $n_{LN:Mg}$ and n_{LN} are the refractive indices of waveguide layer and substrate, respectively, which are related to the temperature. Based on the above equations, we can get the expression of Cherenkov TH angle out of the crystal, as below:

$$\sin\theta_c^{\text{out}} = n_{\text{LN}}(T,3\omega)\cdot\sin \times\left\{\arccos\left[\frac{n_{\text{LN:Mg}}(T,\omega)\cdot k(\omega) + n_{\text{LN:Mg}}(T,2\omega)\cdot k(2\omega) + G_{\text{m}})}{k(3\omega)}\right]\right\} \quad (12)$$

Due to the modulation corresponding to forward reciprocal vectors, $\vec{v_p}$of the non-linear polarization wave are decreased so as to be smaller Cherenkov angles. On the contrary, the modulation corresponding *to* backward reciprocal vectors effectively accelerates the $\vec{v_p}$, which results in larger Cherenkov angles. As shown in figure 5, all the angles of TH radiations at varieties of temperature conditions were calculated via equation (12), which included the cases reciprocal vectors $\vec{G}_{-2}$, $\vec{G}_{-1}$, $\vec{G}_1$, involved and without reciprocal vectors involved. Unlike TH

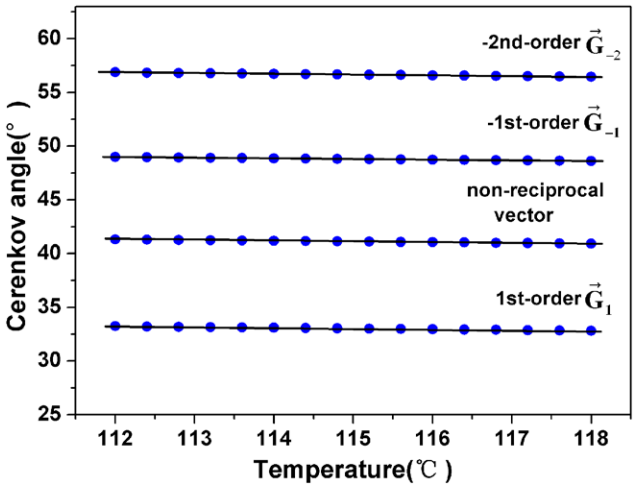

Figure 5. Cherenkov angles vary with temperature for cases when different reciprocal vectors involve in the CTHG process.

intensity, which has a significant relationship with the change in temperature, all the Cherenkov angles almost remain the same and are insensitive to the temperature variation.

For a given pump power density of 0.2 MW cm^{-2} and a temperature of 115°C, the three situations of QPM CTHG were studied, and the dependences of the TH power on interaction length L are shown in figure 6. One could find that at the same interaction length, for the two cases with reciprocal vectors involved, the TH radiation with $\vec{G}_1$ participating always has a larger intensity than that of the case using $\vec{G}_{-1}$. Actually, the modulation to Cherenkov TH depends on the QPM structure in theory. When different reciprocal vectors provided by the structure are involved, distinct modulated effects can be obtained. We derived the efficiency of the generated cascading Cherenkov TH from the coupled mode equations, as in the following:

$$\eta \propto P^2(\omega)\cdot d_{\text{SHG}}{}^2\cdot d_{\text{SFG}}{}^2\frac{|\vec{\beta}(\omega) + \vec{\beta}(2\omega) + \vec{G}_{\text{m}}|}{\rho}, \quad (13)$$

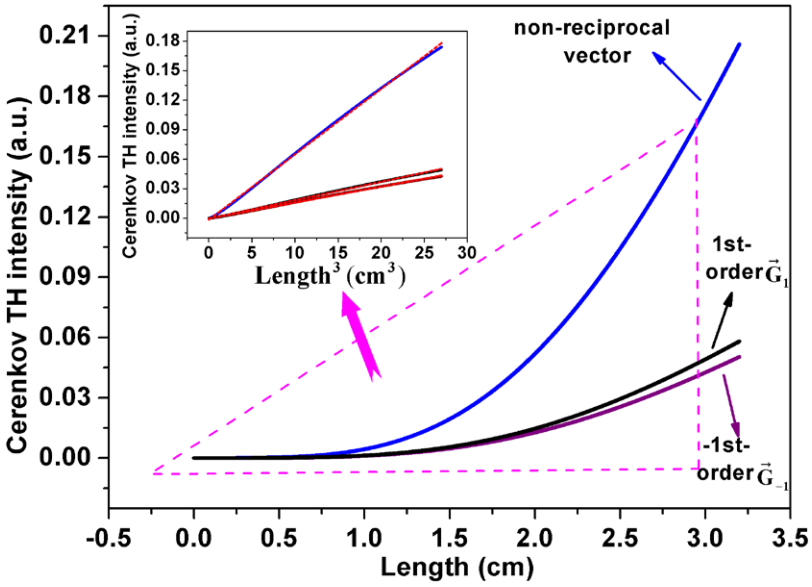

Figure. 6. The simulated results of TH power dependences on interaction length for three situations: forward reciprocal vectors $\vec{G}_1$ involved, without reciprocal vector involved and backward reciprocal vector $\vec{G}_{-1}$ involved. At the top left corner, the inset figure shows the fitting curves of the data in the triangular region.

in which $P(\omega)$ is the power of fundamental wave; d_{SHG} and d_{SFG} are the effective non-linear coefficients of the two cascaded processes, respectively, which are related to the QPM structure; $\vec{G}_m$ is the involved reciprocal vector; and ρ is defined as the wave-number of the corresponding Cherenkov TH. The parameterρincreases with the increase of the Cherenkov angle, so from equation (13), we can see that, for the Cherenkov TH corresponding to a larger Cherenkov angle (the case of backward reciprocal vector involved), the efficiency is smaller. On the other hand, the Cherenkov angle is larger, which leads to a smaller corresponding effective interaction length, so the efficiency of Cherenkov TH should be lower as well.

We define $\mathbf{I^j}$, $1/\gamma_2^j$ and $\mathbf{d}_{\mathrm{eff}}^{\mathrm{j}}$ as TH intensity, the mode-overlapping coefficient and effective non-linear coefficient, respectively, where $j = 0$ represents the case without any reciprocal vectors and $j = \pm 1, \pm 2...$ represents the case using the jth-order reciprocal vector. According to the above analyses, the mode overlapping decreases with the increasing of the Cherenkov angle. In these three situations, TH radiation with $\vec{G}_1$ involved has the smallest Cherenkov angle while radiation with $\vec{G}_{-1}$ involved has the largest one, and the mode overlapping follows $\gamma_2^1 > \gamma_2^0 > \gamma_2^{-1}$. Based on our numerical results in figure 4, γ_2^0 is only a little smaller than γ_2^1, while $\mathbf{d_{eff}^0}$ is much larger than $\mathbf{d_{eff}^1}$. Because $\mathbf{I^j}$ increases with the term $\left(\gamma_2^j\right)^2 \cdot (\mathbf{d_{eff}^j})^2$, the TH intensity may follow $\mathbf{I^0 > I^1 > I^{-1}}$. The calculated relative intensity of each TH radiation, together with corresponding mode overlapping and effective non-linear coefficient, are illustrated in table 1. We could find that the radiation without reciprocal vector participating has the largest intensity, while the intensity of the radiation using $\vec{G}_{-2}$ is the weakest; these findings are in accordance with the above theoretical discussions.

Table 1. The relative values of overlapping (γ_2), efficient nonlinear coefficient ($\mathbf{d_{eff}}$) and intensity ($\mathbf{I}$) for each CTHG spot.

	$\vec{G}_1$	0	$\vec{G}_{-1}$	$\vec{G}_{-2}$
$1/\gamma_2$ **(a.u.)**	1.06	1	0.804	0.161
$\mathbf{d_{eff}}$ **(a.u.)**	0.592	1	0.592	0.0904
I (a.u.)	2.82	10	2.44	0.0764

Based on equations (3)–(5), Cherenkov TH intensity can be expressed as

$$I_{3\omega} \propto I_\omega^3 \cdot L^3 \cdot \left(\frac{\sin\Delta\beta_1 L}{\Delta\beta_1 L}\right)^2 \cdot \kappa_1^2 \cdot \kappa_2^2 \qquad (14)$$

which was deduced via non-depletion approximation of the fundamental wave and the slowly varying envelope of the SH wave. Following equation (14) above, we can see that $I_{3\omega}$ is proportional to the cubic of non-linear interaction length L. It should be pointed out that this characteristic is peculiar to the CTHG process, and is quite different from that of the THG in bulk crystals using the same cascaded $\chi^{(2)}$ processes [21]. As shown in the inset figure at top-left corner of figure 6, when L was less than 3 cm, the simulated curves were well fitted to our theoretical analysis. If L was more than 3 cm, the simulated curves would gradually deviate from theoretical values, because the SHG efficiency became higher as L gradually increased, so the non-depletion approximation cannot be used.

4. Conclusion

In conclusion, we have numerically investigated QPM CTHG, which comprises two cascaded $\chi^{(2)}$ processes in a waveguide following coupled-mode theory. At different pump powers, the temperature-detuning curves of TH are widely different from each other. We also found that the

two sides of the temperature-detuning curves were asymmetric, which is distinct from the bulk THG process. The reason is that the mode overlapping in the CTHG process has a strong relationship with the temperature. The output TH power dependences on interaction length have been discussed as well, which demonstrated that non-depletion approximation is merely available in certain particular conditions. In addition, the Cherenkov angle of each radiated TH was found to be not significantly affected by temperature variation. We believe these characteristics demonstrated in the paper would be of help for further investigations on QPM CTHG and other non-linear Cherenkov processes.

Acknowledgements

This work was supported by Jiangsu Science Foundation (BK2011545), and the National Natural Science Foundation of China under Contract No. 61205140.

References

[1] Tien P K, Ulrich R and Martin R J 1970 *Appl. Phys. Lett.* **17** 447
[2] Li M J, De Micheli M, HE Q and Ostrowsky D B 1990 *IEEE J. Quantum Electron.* **8** 1384
[3] Vaya M, Thyagarajan K and Kumar A 1998 *J. Opt. Soc. Am.* B **15** 1322
[4] Ramponi R, Marangoni M, Osellame R and Russo V 1999 *Opt. Commun*. **159** 37
[5] Deng X W and Chen X F 2010 *Opt. Express* **18** 15597
[6] Wang W J, Sheng Y, Kong Y F, Arie A and Krolikowski W 2010 *Opt. Lett.* **35** 3790
[7] Molina P, de la O Ramirez M and Bausa L E 2008 *Adv. Funct. Mater.* **18** 709
[8] Sanford N A and Connors J M 1989 *J. Appl. Phys.* **65** 1429
[9] Yamamoto K, Yamamoto H and Taniuchi T 1991 *Appl. Phys. Lett.* **58** 1227
[10] Chen C D, Su J, Zhang Y, Xu P, Hu X P, Zhao G, Liu Y H, Lv X J and Zhu S N 2010 *Appl. Phys. Lett.* **97** 161112
[11] Zhang Y, Gao Z D, Qi Z, Zhu S N and Ming N B 2008 *Phys. Rev. Lett.* **100** 163904
[12] Sheng Y, Best A, Butt H J, Krolikowski W, Arie A and Koynov K 2010 *Opt. Express*. **18** 16539
[13] Chen C D, Hu X P, Xu Y L, Xu P, Zhao G and Zhu S N 2012 *Appl. Phys. Lett.* **101** 071113
[14] Chen C D, Lu J, Liu Y H, Hu X P, Zhao L N, Zhang Y, Zhao G, Yuan Y and Zhu S N 2011 *Opt. Lett.* **36** 1227
[15] Sheng Y, Wang W J, Shilon R, Roppo V, Kong Y F, Arie A and Krolikowski W 2011 *Appl. Phys. Lett.* **98** 241114
[16] An N, Ren H J, Zheng Y L, Deng X W and Chen X F 2012 *Appl. Phys. Lett.* **100** 221103
[17] Li H X, Mu S Y, Xu P, Zhong M L, Chen C D, Hu X P, Cui W N and Zhu S N 2012 *Appl. Phys. Lett*. **100** 101101
[18] Tamada H 1991 *IEEE J. Quantum Electron.* **27** 502
[19] Hayata K, Matsumura H and Koshiba M 1991 *J. Appl. Phys.* **70** 1157
[20] Dmitriev V G, Gurzadyan G G and Nikogosyan D N 1999 *Handbook of Nonlinear Optical Crystals* (New York: Springer)
[21] Ivanov R, Koynov K and Saltiel S 2002 *Opt. Commun.* **212** 397